Geospatial investigation of physico-chemical properties and thermodynamic parameters of biomass residue for energy generation

Obafemi O Olatunji[1*], Stephen Akinlabi[2,3], Nkosinathi Madushele[1], Paul A. Adedeji[1], Matumuene J. Ndolomingo[4]

[1]Department of Mechanical Engineering Science, University of Johannesburg, South Africa
[2]Department of Mechanical and Industrial Engineering, University of Johannesburg, South Africa
[3] Department of Mechanical Engineering, Walter Sisulu University, South Africa.
[4]Department of Chemical Sciences, University of Johannesburg, South Africa

[*]*Corresponding author: tunjifemi@gmail.com*

Abstract

Biomass represents vast under-explored feedstock for energy generation across the globe. Among other factors, the location from where the feedstock is harvested may affect the overall properties and the efficiency of bio-reactors used in the conversion process. Herein is reported some physicochemical properties, the kinetic study and thermodynamic analysis of corn cob sourced from two major economies in sub-Sahara African region. Brunauer Emmett and Teller (BET) analysis was performed to investigate the surface characteristics of corn cob while Fourier Transform Infrared Spectroscopy (FTIR) revealed the corresponding functional group present in the selected biomass residue. The proximate and CHNSO analyses were performed using the standard equipment and following the standard procedures, then the result is reported and compared based on the geographical locations under consideration. Also, the thermal decomposition study was carried out at different heating rate (10, 15, 30 $Cmin^{-1}$) in inert atmosphere while the kinetic parameters were evaluated based on Flynn–Wall–Ozawa (FWO), and Kissinger–Akahira–Sunose (KAS) methods The Analysis of variance (ANOVA) showed that there is a statistically significant difference between ultimate constituents, the fixed carbon, and volatile matter obtained from the two countries at 95% confidence level. FTIR showed different spectra peak in both samples which means there are varying quantity of structural elements in each feedstock. The pore surface area (1.375 m^2/g) obtained for corncob from South Africa (SC25) was greater than the value (1.074 m^2/g) obtained for Nigeria (NC25). From the result, the highest value of activation energy, (E_a =190.1 $kJmol^{-1}$ and 189.9 $kJmol^{-1}$) was estimated for SC25 based on KAS and FWO methods respectively. The result showed that geographical location may somewhat affect some energetic properties of biomass and further provides useful information about thermodynamic and kinetic parameters which could be deployed in the simulation, optimization and scale-up of the bioreactors for pyrolysis process.

Keywords: Corn cob, Geospatial investigation, Physicochemical properties, Power generation, Pyrolysis, Thermodynamic parameters.

1. Introduction

The deleterious consequences of unabated consumption of fossil fuel are too enormous to be ignored. As of year 2018, the world population was estimated at 7.63 billion [1]. It is obvious that the fossil fuel may not be able to support the energy demand of the emerging population, which is growing at an exponential rate [2-4]. Apart from the population issue, the by-products generated from fossil fuel breakdown during its use are very harmful to the environment and have been heavily implicated in greenhouse gas (GHG) emission [2]. Global decarbonization which is at the centre of Paris agreement on climate change can be achieved through the expansion of renewable energy technologies [5-7]. Consequentially, it has been saddled on all the economic sectors to evolve green and clean strategies in support of environmentally-friendly energy resource generation in order to halt further damages to our planet while reducing the carbon emission. Interestingly, the evidence across the globe has largely been positive toward the capability of the renewable energy sector to play a vital role in regional socio-economic

development. More so, the implementation of integrated renewable energy (RE) resources across many regions offers opportunity for regional energy development and job creation if all the related logistics and diplomatic criteria are well addressed.

While the future energy mix which would provide the needed RE is a nexus of sources, biomass fuel promises to play a significant role. Generally, affordable, dependable, sustainable and modern energy, implies energy availability in various forms (liquid, solid, gases) and ready for use in different sectors of the economy. This is where the overarching benefits of biomass are highlighted. For instance, there is no evidence yet to prove that wind energy can directly replace the aviation fuel, while the intermittency and uncertainties related to solar energy may not position it as the immediate substitute, though with the advance in research and technologies, we cannot rule out such in the future. Biomass is positioned as the main entry point by which substantial renewable energy generation can be sustainably accomplished in order to ensure inclusive energy access. According to IEA latest market forecast [29], modern bioenergy will account for the highest growth in RE between 2018 and 2023, this further highlight the critical role of biomass in the development of robust RE portfolio. Biomass has the potential in making a giant stride towards carbon-neutral chemical and fuel production. It can be converted to two energy-related products, which are transportation fuels and heat [8]. The fuel generated, especially from the agricultural residue and the other third generation biofuels [9] can be applied in electricity generation, transportation, heating and cooling across all the economic sectors of the society, considering criteria such as energy efficiency, applicability, environmental impact, and flexibility. Biomass can be sourced from agricultural residue, energy crop, energy grasses, wood residue, forest residue, and municipal waste [10, 11].

In the developing countries, the application of biomass has shown promises towards the improvement of bioenergy generation. Among the developing countries in Africa, sub-Saharan region which currently hosts the two largest economy (Nigeria and South Africa) in the continent are well known as one of the largest hub in agricultural production, and biomass has been their main source of energy since the ancient time [12-14]. As at 2018, the gross domestic product (GDP) of Nigeria and South Africa were estimated at 397 and 366 billion USD respectively [15]. The agricultural residue generated in Nigeria was estimated at 145.62 MT as of 2013 [16] while agricultural practices contributed 0.8 % of 3.1 % economic growth which was experienced by South Africa in the last quarter of 2017. From these countries, much residue is generated from corn, which makes corn cob very abundantly available. Corn cob is a part of above-ground material of the corn which are left after the grains have been removed. It has been previously classified as a waste since its economic value was not well understood. But recent development has led to its improved use in support of bioenergy generation toward the reduction of fossil fuel dependency [17, 18]. Globally, as at 2017, 7.42 % of corn produced is from Africa (Table 1) with 16.82 MT and 10.42 MT from South Africa and Nigeria respectively (Figure 1).

Table 1. Annual corn production in the world and Africa between 2000-2017 [19]

Year	Africa (MT)	World (MT)	% Africa
2000	43.8	592.0	7.40
2001	41.4	615.2	6.74
2002	45.0	603.6	7.45
2003	45.6	645.1	7.07
2004	48.3	729.5	6.62
2005	50.4	714.2	7.05
2006	50.2	707.9	7.09
2007	48.4	792.7	6.11
2008	58.4	829.2	7.04
2009	60.0	820.1	7.32
2010	66.2	851.7	7.78
2011	65.9	886.7	7.43
2012	71.9	875.0	8.21
2013	71.1	1,016.2	7.00
2014	79.1	1,039.3	7.61
2015	73.6	1,052.1	6.99

2016	73.5	1,100.2	6.68
2017	84.2	1,134.7	7.42

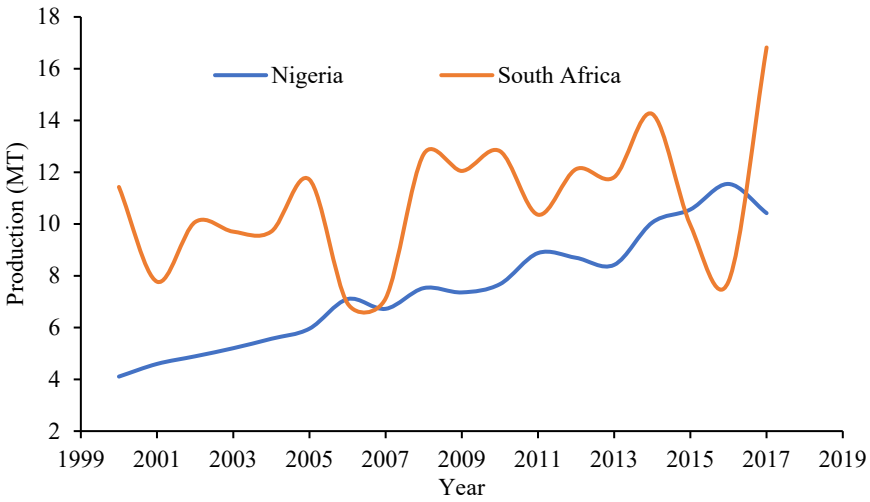

Figure 1. Corn production in Nigeria and South Africa between 2000-2017 [19]

In overall, regional planning of biomass from different geospatial locations could be of advantage to national planning and the achievement of regional emission reduction target while addressing the wider concerns related to bioenergy production. Indeed, biomass footprint in a country should take cognizance of the consequential effect on the neighbouring countries. But, there is a general agreement by the research community that biomass feedstock variability is the root cause of many technical challenges hampering the global commercialization of integrated biorefinery, IBR [20]. These variability which affect the properties of biomass include; climatic condition and season of the year, age of plant, transport and storage condition, soil type, geospatial components and tillage treatment so on [21-25]. Therefore, the properties of the biomass feedstock need to be understood for a successful utilization in energy generation. Specifically, the conversion of biomass to energy is contingent on the understanding of the constituents and various properties which can impact the techno-economic suitability and enhance the development of modern and efficient conversion technologies. Several authors have investigated the ultimate, proximate and the heating value of corn cob [18, 26-28]. Most recently, Djatkov *et al.* [28] investigated the parameters that influence the mechanical-physical properties of pellet fuel made from corn cob and Mostafa *et al.* [27] follow up with a similar analysis on the significance of the pelletization operation conditions. The authors are not aware of any study which have investigated the geospatial effect on surface properties, and functional groups of corn cob. The most recent investigation which considered the surface area (though not on geospatial basis) was carried out by Leal *et al* [20], and this was only limited to corn stover and not corn cob, which is a component of corn stover. In order to facilitate an informed choice of biomaterial for energy generation, the physicochemical properties which include the crystalline phases, surface area, the pore sizes, and the functional group, attributed to a feedstock, need to be well understood. Also, the knowledge of thermal decomposition of bioenergy feedstocks and thermodynamic parameters are of high significance in the conversion of biomass and the development of reactors in a large scale pyrolysis process [29]. Thermodynamic parameters provide a useful engineering tools which can be applied to the thermal conversion process and are useful in the feasibility assessment [30, 31].Although the kinetics of biomass and the thermodynamic parameters have been studied by some research groups [29, 31-35], there is a need to further investigate the thermodynamic parameters of corn cob while also drawing a comparison on the geospatial basis.

There has been advocacy for regional integration of bioresources. For instance, clustering and energy integration have recently emerged in the field of biomass energy supply chain. This motivated Lam et al. [36] to propose regional clustering approach in biomass resources integration using a novel regional energy clustering (REC) algorithm Also, several studies have discussed regional integration of biomass with focus on supply chain management [36-39]. Biomass belong to the mainstream of Europe bioeconomy strategy which was adopted in 2012 and revised in 2018 [40], and has been a popular trade commodity across the countries in this region [41]. Interestingly, biomass from agriculture is the main driver of the overall biomass trade and the growth in its demand has caused a substantial rise in the volume of international trade. Further down in the southern hemisphere of Africa, Southern Africa Development Community (SADC) made provision for the utilization of RE through

regional integration and development of renewable energy resources. This RE resources include biomass which substantially emanate from agricultural practices which forms one of the major parts of their economy [42]. Authors are not aware of any study which have carried out a geospatial comparison of the properties of corn cob from Nigeria and South Africa. Yet, the effect of geospatial component on the feedstock properties needs to be clearly understood, to provide a first-hand knowledge of the dynamics of biomass resource integration from different geographical locations with significant longitudinal and latitudinal variances. In view of this and based on the motivated possibility of regional integration of bioresources, this study (i) investigates the physicochemical properties of corn cob sourced from Nigeria and South Africa, (ii) evaluates the thermal decomposition and estimates the thermodynamic parameters of corn cob sourced from Nigeria and South Africa, (iii) and finally compares the experimental results obtained from each country. The rest of this study is sectioned as follows: section 2 discusses the materials and methods used in this study, section 3 presents the results obtained and further discusses the findings in this study and finally, section 4 presents the conclusions to this investigation.

2. Materials and methodology

2.1. Biomass sampling and pre-treatment

Corn cob was acquired from two geospatial location; the first in Tshwane municipality in Gauteng province, South Africa (25° 52' 48.95" S, 28° 22' 33.16" E) in November 2018 and the second in Ile-Ife, Osun State, Southwest of Nigeria (7° 17' 0" N, 4° 28' 0" E) in April 2018 using purposive sampling technique. The samples were gathered at different months because the peak period for corn production was different for the two countries. The biomass residue was air-dried for seven days in an open-air and then further dried in an oven at 45 ^{0}C for 48 h. The earth and other contaminants were removed manually to avoid external influence on the results as much as possible. The samples were manually downsized to around 1 cm using a knife and then stored in an air-tight Ziplock bag. Further to this, the dried biomass was pulverized using vibratory disk milling machine. The particles were sieved to sizes passing < 250 μm. The sieved samples were stored in an air-tight bag and kept in a desiccator at room temperature.

2.2. *Experimental procedure*

This section describes the experimental methods and procedures which were adopted in this study. In order to determine the feasibility of corn cob feedstock for energy generation, the characterization of the feedstocks was based on several physicochemical parameters which may have significant effect on the conversion pathway of biomass fuel [21]:

- *The proximate analysis*, which includes percentages of volatile matter (VM), fixed carbon (FC), and ash content (Ash).
- *Ultimate analysis* to determine the carbon, C, hydrogen, H, oxygen, O, sulphur, S, nitrogen, N content. These elements are the major component of biomass and they determine its fuel efficacy and gross contribution to greenhouse gas emission (GHG) to a large extent.
- *The high heating value (HHV*), which was determined experimentally using eco-bomb calorimeter and empirically using some existing empirical relation in the literature.
- *Brunauer Emmett and Teller (*BET) analysis to determine the particle size distribution, pore surface area and volume.
- *X-ray Diffraction Analysis (XRD)* analysis to determine crystal phases of various biomass samples
- *Fourier Transform Infrared Spectroscopy (FTIR)* to understand the presence and distribution of different function groups
- *Thermogravimetric (TG)* analysis to investigate the devolatilization characteristics and variation for different biomass samples

Table 2 shows the measuring equipment and the standard deviation with associated physicochemical parameters which were measured. Based on the number of parameters which were investigated the total number of samples are seventy-two (72) with thirty- six (36) each for SC25 and NC25.

Table 2. Biomass properties and measurement equipment with standard deviation

Parameter	Units	Measuring equipment	Standard deviation	Number of replications
Volatile matter	%	Thermolyne Furnace 6000	0.02	3

Fixed carbon	%		0.02	3
Ash	%		0.02	3
Carbon, C	%		0.12	3
Hydrogen, H	%	Thermo scientific FLASH	0.03	3
Nitrogen, N	%	2000 CHNS analyser	0.009	3
Sulphur, S	%		0.002	3
HHV	MJ/kg	Cal2k Eco calorimeter	0.02	3
TG analysis	%	STA 7200V TG Analyser		3
Pore size Pore volume Pore surface area	nm cm^3/g m^2/g	Micromeritics ASAP2460	0.001	3
FTIR (Transmittance peak)	%T	IRAffinity-1S	0.02	3
XRD	arb	Rigaku miniflex	0.02	3
Total number of sample				**36**

2.2.1 Proximate analysis

The proximate analysis of biomass was obtained based on the ASTM standards [43-48]. All the proximate analysis were carried out under controlled temperature, time, weight, and equipment in compliance with ASTM E1755-01 [48]. The experiments were performed in triplicate to ensure repeatability. The moisture content of biomass samples was estimated with a convection furnace based on the procedure prescribed in ASTM [45]. The high-temperature alumina crucible was first heated at 105 ± 3℃ for 3hrs; it was then removed and allowed to cool down to room temperature inside the desiccator and the weight, w_c was recorded. The 3g of the sample were added to the crucibles and the weigh, w_i was recorded. The crucibles were heated in a controlled atmosphere at 105 ± 3℃ for 24hrs then removed and allowed to cool down to room temperature in the desiccator. It was then weighted to the nearest 0.1mg. The sample were place back in the furnace at the same temperature until constant weight, w_f was attained. Then the moisture and total solid content was calculated as follows:

$$Moisture, M(\%) = \frac{(w_i - w_c) - (w_f - w_c)}{w_i - w_c} \times 100 \quad (1)$$

The volatile matter is the fraction of moisture-free content that evolved when biomass is heated to high temperature in an inert atmosphere. The volatile matter that is released during the heating process may be from inorganic source and organic source. The design of biomass power plant and thermal decomposition can be affected by the volatile matter since high volatility promotes low-temperature fuel ignition which can impact efficiency of a combustion process [49]. The moisture-free sample was heated for 7mins at 950 ± 10℃ in the absence of air. The crucible was then removed and allowed to cool in the desiccator. The weight of the crucible with sample after 7mins of heating, w_{f950} was recorded. Then the volatile matter, VM was calculated on dry basis as follows;

$$volatile\ matter, VM(\%) = \left[\frac{(w_i - w_c) - (w_{f950} - w_c)}{w_i - w_c} \times 100\right] - M(\%) \quad (2)$$

The ash content is detrimental to the pyrolysis process since the deposits on the boiler tube could decrease the heat transfer. In addition, a high percentage of ash could increase the logistic cost such as; maintenance, transportation, ash treatment, dust emission and so on. Ash content affects the rate of pyrolysis of the biomass sample. In order to determine the ash content, the biomass sample was measured into the crucible and then placed in the furnace which was maintained at 575±10 ℃ for 3 hrs. The crucible was then removed and placed in the desiccator to cool down. The weight, w_{f575} of the crucible with sample after 3 hrs of heating was then recorded. The process was repeated until the constant weight was obtained. The repetition was to allow the removal of all remaining volatile and unburnt carbon. The weight difference gives the ash content [50].

$$Ash\ Content, Ash(\%) = \frac{(w_{f575} - w_c)}{w_i - w_c} \times 100 \quad (3)$$

The fixed carbon provides information about the optimum resident time for a complete process. The fixed carbon content (FC) was calculated based on the expression as given in Eq. (4).

$$FC(\%) = 100 - (\%VM + \%A) \quad (4)$$

where FC, VM, are proximate values for fixed carbon content and volatile matter on dry basis.

2.2.2 Ultimate analysis

The Elemental analyser was used to determine the ultimate properties of corn cob samples. Prior to the analysis, the elemental analyser was calibrated using 5 tins capsules packed with a 5L-cystine test, with 0.1mg biomass samples in each capsule. The milled biomass sample of 0.1mg by weight was added to a tin capsule and then heated to 980^0C with a continuous supply of helium- enriched oxygen gas. The data obtained through this process was then analysed in order to determine the elemental composition of the biomass. The weighted percentage of carbon C, hydrogen H, sulphur S, nitrogen N were determined, and the percentage of oxygen O was determined based on the mean difference:

$$O(\%) = 100 - (C + H + N + S) \quad (5)$$

2.2.3 Heating value

The heating value of a fuel is defined as the energy evolved per unit volume of the fuel during a complete combustion process. When all the moisture content is condensed out of a combustion sample, the high heating value HHV is obtained. The HHV of the biomass samples were determined using calc 2k Eco bomb calorimeter [51]. The Cal2k Eco calorimeter consist ; the calorimeter, filling station, and vessel. The vessel which hold the sample is filled with compressed air at 3000kPa and 25^0C at the filling station, before firing inside the bomb calorimeter. Cal2k Eco calorimeter requires the ancillary components which include; the gas defiller cap, pressure gauge, cotton, crucible, scale balance, firing wire, and electrode. The vessel was first calibrated before the testing, corn cob sample of 0.5g was then used for each test. A cotton thread was attached to the platinum ignition wire and submerged in the sample. The pressurized vessel was placed in the bomb calorimeter and the lid was closed as prompted. After the calorific value of the sample is displayed, the vessel was removed and outgassed. The HHV was validated using empirical correlations which have been previously developed based on the ultimate and proximate analysis. The tests were performed in triplicates in order to ensure the reliability of the result and the average result was presented.

2.2.4 Fourier Transform Infrared Spectroscopy (FTIR)

FTIR has evolved as a method which can be applied to explain the structure and functional groups which may be present in the biomass. It is a non-destructive method used for qualitative and quantitative estimation. The functional groups inherent in the corn cob was characterized with PerkinElmer FT-IR spectrum GX specification. 10 mg dry sample was thoroughly mixed with 200 mg KBr and compressed to form pellets. The spectra were obtained at a total scan time of 20 sec within the infrared (IR) range of 400-4000 cm^{-1} at 1 cm^{-1} step size. Table 7 shows the most prominent functional group and the wavenumber.

2.2.5 Brunauer Emmett and Teller (BET) Analysis

This method was invented by three scientists; Stephen Brunauer, P.H Emmet and Edward Teller in the year 1938 [52]. It is built on the principle of desorption and adsorption of a gas on the surface of materials. The amount of gas which is adsorbed and releases at a specific pressure is the basis for the determination of pore surface area. It is a cheap, fast and dependable method which has gained application in many fields [52-54]. The probing gas for this process is selected in such a way that there is no reaction between the material surface and the adsorbate gas that is used to determine the specific surface area. It is important to understand the surface characteristics of biomass since it has effect on solid handling and transportation [20]. BET measurements were achieved using a Micromeritics ASAP2460 surface area and porosity analyser. Before this analysis, milled corn cob was degassed with nitrogen at 90 ^{0}C for 12 h. It is worth noting that the sample mass before and after degassing was less than 0.005 g; which shows that the sample was relatively moisture-free during the transferring, weighing, loading and unloading operations. Proper sample drying was a critical factor in obtaining reliable results in specific surface area (SSA) measurements. Re-uptake of moisture in samples was mitigated by immediately placing a rubber stopper over analysis tube while weighing and transferring to the instrument. All the measurements were carried out at −196 °C. The pore volume, pore surface area, and pore sizes were calculated from the adsorption curves using the Barrett-Joyner-Halenda (BJH) model [20, 55].

2.2.6 X-ray Diffraction Analysis (XRD)

An understanding of the phases of a biomass and the data on the cell component can be obtained from X-ray Diffraction, XRD. In this case, the finely grounded corn cob sample was scanned through ranges of 2θ angles so as to achieve all possible diffraction routes. For the XRD analysis, the milled biomass samples were analysed using Rigaku mini flex 600 powder diffractometer which is equipped with Cu Kα radiation source generated at 18 kW and 250 mA. The XRD spectra were obtained at a room temperature. High angle, HA measurement was performed at a range of 2θ =10-50 ^{0} at a step rate of 0.4 ^{0}/min, since the most significant result was obtained within this range. Three spectra were considered for each of the replicated sample. The XRD pattern which was obtained was processed with Match! Version 2 software package [56].

2.2.7. Thermogravimetric (TG) Analysis

In order to study the kinetics of corn cob NC25 and SC25 under pyrolysis conversion condition, the simultaneous thermal analysis (STA) was performed. This techniques is the combination of thermogravimetric analysis and differential scanning calorimetry under a controlled atmosphere which is inert (nitrogen) atmosphere in this study [35]. In order to eliminate system errors, the baseline against which the TG curves were corrected was first established. Also, each heating rate was performed three times to ensure the repeatability of the experiment within 2% error margin. Since the solid-state kinetic data is of major interest in thermal processes, the kinetic parameters such as activation energy E_a and pre-exponential or frequency factor k_0 were obtained using iso-conversion solid-state kinetics [32, 33]. Generally, pre-exponential factor is related to the entropy of the interacting molecules with the accompanied reactions. Also, E_a is defined as the minimum amount of energy required to initiate a chemical reaction. It means that these two parameters are used to determine if there is a possibility of reaction in the pyrolysis of corn cob and at what minimum energy will this reaction be initiated. Specifically, there is an inverse relationship between the rate of pyrolysis and the activation energy.

Two kinetics models which are Flynn–Wall–Ozawa (FWO), Kissinger–Akahira–Sunose (KAS) were evaluated in order to determine the activation energy and the frequency factor for NC25 and SC25. The reaction rate is a function of change in conversion per unit time and it is a function of the conversion rate, α, given in Eq. (7) such that;

$$\frac{d\alpha}{dt} = k_0(T)f(\alpha) \tag{6}$$

The $f(\alpha)$ is the model of reaction for heterogenous conversion process and reaction constant $k_0(T)$ is fundamentally governed by Arrhenius equation, which is an indication of the effect of temperature on the rate of reaction. Therefore, conversion degree α and $k_0(T)$ can be expressed as Eq.(7) and Eq.(8):

$$\alpha = \frac{m_0 - m_t}{m_0 - m_\infty} \tag{7}$$

where m_0 is the initial mass, m_t is the mass at the time t and m_∞ is the final mass of the residue as recorded using weigh balance.

$$k_0(T) = k_0 e^{-\frac{E_a}{RT}} \tag{8}$$

where k_0 is the pre-exponential Arrhenius factor, E_a is the activation energy, T is the absolute temperature (K). Assuming that temperature is a function of time and increases with a constant heating rate β(℃ min^{-1}), then β is given as Eq. (9)

$$\beta = \frac{dT}{dt} = \frac{dT}{d\alpha} \times \frac{d\alpha}{dt} \tag{9}$$

Therefore, based on Eq. (8) and (9); Eq. (10) is generated thus;

$$\frac{d\alpha}{dT} = \frac{k_0}{\beta} e^{-\frac{E_a}{RT}}.f(\alpha) \tag{10}$$

The combination of Eqs. (9) and (10) can be expressed as Eq. (11);

$$g(\alpha) = \int_0^{\alpha} \frac{k_0}{\beta} e^{-\frac{E_a}{RT}} dT = \frac{k_0 E_a}{\beta R} \int_y^{\infty} v^{-2} e^{-v} dv = \frac{k_0 E_a}{\beta R} P(y) \quad (11)$$

where $g(\alpha)$ represent the integral form of the reaction model and $P(y)$ is an approximated temperature integral equation, with $y = \frac{E_a}{RT}$. It is noted that Eq. (11) does not have exact solution, therefore an approximated solution for this integral expression is used on the development of isoconversion methods. The approximation equation of Doyle and Murray-white are respectively associated with FWO and KAS methods [31].
Given that $y = \frac{E_a}{RT}$ and the function $P(y)$ is non-exact solution, rearrangement and approximation of Eq. (11) with $P(y) = y^{-2}e^{-y}$ is an expression of KAS method [57, 58] Eq. (12) while FWO method Eq. (13) is derived based on Doyle's approximation [59].

$$\text{KAS: } ln\left(\frac{\beta}{T_p^2}\right) = ln\left(\frac{k_0 E_a}{R g(\alpha)}\right) - \left(\frac{E_a}{RT}\right) \quad (12)$$

$$\text{FWO: } ln\beta = ln\left(\frac{k_0 E_a}{R g(\alpha)}\right) - 1.052\left(\frac{E_a}{RT}\right) - 5.331 \quad (13)$$

2.2.8 Estimation of thermodynamic parameters
The theoretical equation which were derived from activation complex theory (Eyring theory) based on activation energy and frequency factor were used to estimate the thermodynamic parameters [34]. Thermodynamic parameters are represented by change in Gibbs free energy ΔG, enthalpy ΔH, and entropy ΔS and it is presented in Eqs. 11-13 below:

$$\Delta G = E_a + RT_p ln\left(\frac{k_B T_p}{h k_0}\right) \quad (14)$$

$$\Delta H = E_a - RT \quad (15)$$

$$\Delta S = \left(\frac{\Delta H - \Delta G}{T_p}\right) \quad (16)$$

The ΔG signifies the available energy of in system, ΔS signifies the degree of disorderliness while ΔH represents the differences between the energy of the reagent and the activation complex. T_p is the maximum peak temperature observed from differential thermogravimetric curve (DTG), h is the plank constant which is given by 6.626×10^{-23} J.s and k_B is the Boltzmann constant 1.381×10^{-23} JK^{-1}.

3. Results and Analysis

3.1. Ultimate and proximate analyses
The information about the ultimate constituents, volatile matter (VM), ash content (Ash), fixed carbon (FC) and HHV of corn cob were obtained and presented in Table 3. Nigeria and South Africa were presented alongside some other countries. The analysis of variance (ANOVA) of ultimate constituents for geospatial locations at 95 % confidence level showed that there is a statistically significant difference between the mean value of the ultimate constituents ($p = 4.53 \times 10^{-15}, F = 1016.6 > F_{crit} = 3.259$). Therefore, it can be concluded that the ultimate properties may be affected by the geospatial location from where the corn cob was sourced. Further review of the variance showed that only significant difference in the elemental composition was between the S, O and C content. More so, there is a statistically significant difference between the mean value of the proximate constituents ($p = 1.46 \times 10^{-6}, F = 261.7 > F_{crit} = 5.143$) with the greatest variation observed between the FC, and VM. These result were further compared with Bijoy et al. [60] and Demirbas et al. [61].

The lowest value of H/C was obtained for NC25 while the lowest value of O/C was observed for Demirbas et al. [61]. The lower O/C is an indication of higher energy content since the sample with lower O/C has greater energy content and higher heating value. This is due to stronger chemical bonding between C-C than in O-C bonds [62].

The higher Ash obtained by Bijoy et al. [60] may reduce the heating efficiency since the ash deposit on the boiler tube will decrease the heat transfer. From another perspective, the higher Ash may be beneficial as it may be used as a catalyst in thermal conversion technologies [63]. There are several geospatial based factors which may have accounted for the disparities observed in these properties, these include; the varying local climatic condition, soil and planting condition, fertilizer requirement and so on. Moreover, the feedstock was gathered at different time of the year which coincide with the peak planting period in these countries [8, 21].

Table 3: Comparative analysis of the Ultimate and Proximate properties of corn cob on dry basis

Corn cob	**NC25**	**SC25**	**Demirbas et al. [31]**	**Bijoy et al [33]**
Location	Osun state Nigeria	Gauteng province South Africa	Turkey	Dehradun district India
FC	8.00±0.3	5.50±0.29	18.54	6.54
VM	90.40±0.1	93.20±0.1	80.10	91.16
Ash	1.60±0.08	1.30±0.07	1.36	2.30
C	46.20±0.2	44.80±0.2	46.58	42.10
H	5.40±0.1	5.50±0.1	5.87	5.90
O	47.90±0.1	48.60±0.1	45.46	51.02
S	0.20±0.001	0.79±0.001	0.01	0.48
N	0.30±0.01	0.31±0.01	0.47	0.50
HHV(MJ/kg)	18.70±0.25	18.50±0.27	18.77	16.00
H:C	1.39	1.46	1.50	1.67
O:C	0.78	0.81	0.73	0.91

The results obtained from the experiment was compared with two empirical relations based on the elemental composition and proximate value as presented in Table 4 and 5. The proximate analysis-based empirical relations was closer to the experimental value obtained in this study compared to the relations based on the elemental analysis.

Table 4. Estimated heating value based on Ultimate analysis

	HHV(MJ/kg)		
	NC25	SC25	Max dev
Channiwala and Parikh **[64]**	26.90	27.00	9.00
Demirbas et al. **[65]**	29.60	29.60	11.70
Present study	18.70	18.50	0.00

Table 5. Estimated heating value based on Proximate analysis

	HHV(MJ/kg)		
	NC25	SC25	Max dev
Parikh et al. **[66]**	16.90	16.50	-1.00
Demirbas et al. **[65]**	16.40	16.00	-1.50
Present study	18.70	18.50	0.00

3.2. BET analysis

The results of the surface properties are presented in Table 6. The pore surface area obtained for NC25 and SC25 were in good agreement with literature values [20, 67, 68]. The pore surface area obtained for SC25 was greater than the value obtained for NC25 for the same particle size (250 μm). ANOVA was carried out to further show the impact of the geospatial location on the surface properties of corn cob and the impact of interaction between variables that define the surface properties. At 95 % confidence level, the statistical difference between SC25 and NC25 was significant ($p = 0.00556, F = 46.2911 > F_{crit} = 9.5521$). Further investigation showed a significant variation between the parameters that define the surface properties of corn cob. Pore size was found to show the greatest variation while the pore volume showed the least. Interestingly, pore sizes have a consequential effect on the pore surface area and the pore volume. From the storage life and bioavailability point of view, SC25 showed better behaviour, given its lower pore size which could enhance storage life, bioavailability and transportability [69]. It should be noted that there is a tendency that the observed surface area may be lower than the actual due to a likelihood of microstructure collapse attributable to the drying and freezing during analysis. Figure 2 shows the isotherm plot. The adsorption isotherm does not display any significant broad hysteresis loop since there is close matching between the adsorption and desorption process [70, 71]. Although similar isothermal pattern was obtained for the two feedstocks (NC25 and SC25), the quantity of gas absorbed were different between the relative pressure of 0.5-0.9.

Table 6. Surface properties of corn cob obtained.

Biomass feedstock	Particle size ($\boldsymbol{\mu m}$)	Pore volume (cm^3/g)	Pore surface area (m^2/g)	Pore size (nm)
NC25	250	0.006713	1.074	24.9961
SC25	250	0.006445	1.375	18.7473
SD		±0.0001	±0.05	±0.4

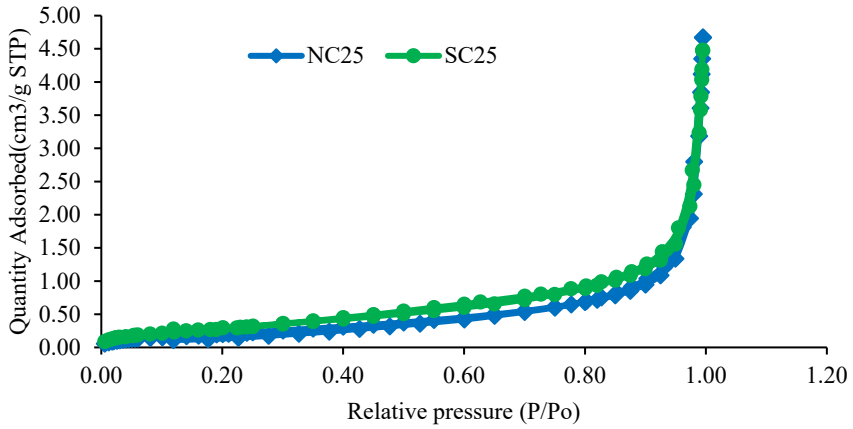

Figure 2: N_2 sorption isothermal plot for corn cob

As a further indication of the distribution of surface properties within a particular sample , pore size distribution for corn cob was presented in Figure 3. There was a close agreement between the pore size distribution obtained for the two feedstocks. This is expected since the particle was ground to the same sizes and under the same grinding conditions.

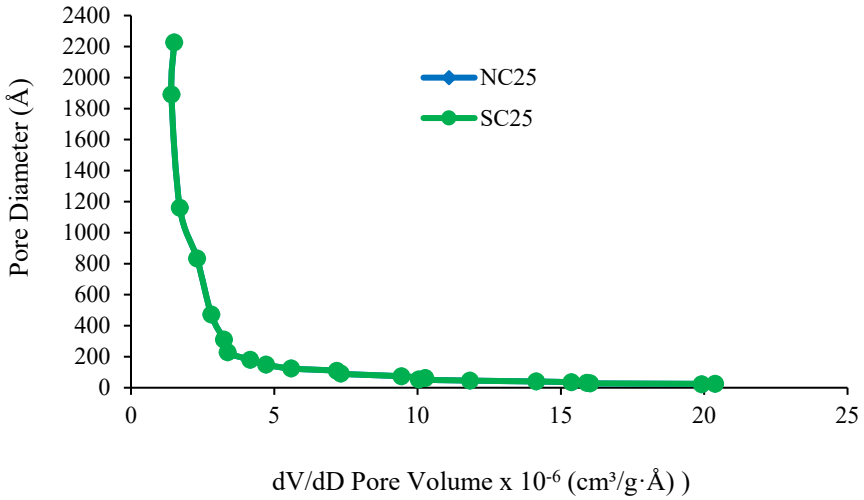

Figure 3: Pore size distribution for corn cob

3.3. Fourier transformation-infra red spectroscopy (FTIR) for corn cob

FTIR has been widely employed to study either the individual component or the structure of biomass. The band position and bond types were obtained from the IR spectrum table and chart [10, 72]. The FTIR spectra of the corn cob samples are shown in Figure 4. Ranges of peaks which correspond to different functional groups were observed in the feedstocks. Different combination of structural carbohydrates (cellulose, hemicellulose and lignin) were observed. Table 7 shows the peak position and the corresponding function group relevant to this study. The major peak at A2 and B2 from 990 to 1035 cm^{-1} is caused by C-O valency vibration, C-O, C=C and C-C-O stretching. The broad peak observed at A6 and B6 (3200-3750 cm^{-1}) is due to O-H stretching and mainly represent of Phenol carboxylic acid and water impurities [10, 73]. All the peaks observed in the two feedstocks fall within the same band position, meaning that the same functional ground can be found in both NC25 and SC25 from Nigeria and South Africa respectively. However, the spectra peaks were different along some band positions (A1 and B1, A2 and B2, A4 and B4, A5 and B5, A6 and B6, A7 and B7) in both samples. This implies that despite a similar functional groups, the composition of the structural elements is different. For instance, the OH stretching found in NC25 is closer to the upper limit of the band compared to the SC25.

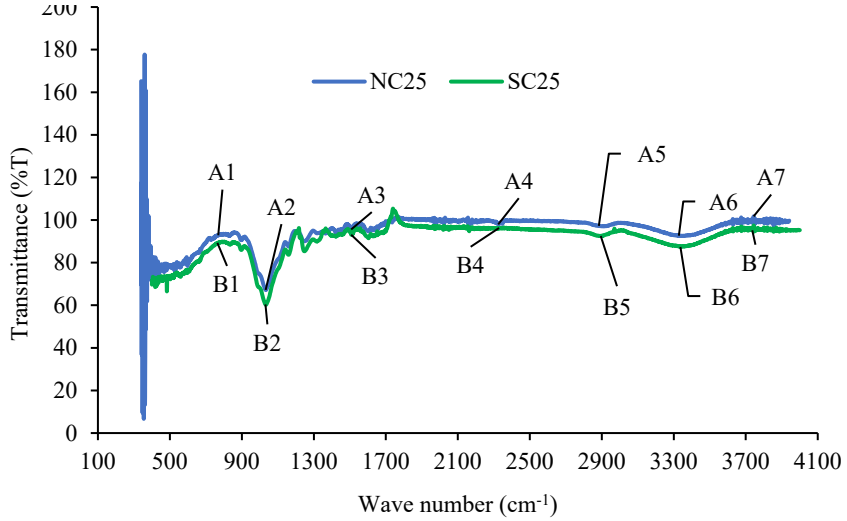

Figure 4: FTIR spectra of corn cob showing different peaks

Table 7: Prominent peak in FTIR analysis of NC25 and SC25

	B-Observed Peak-SC25 (cm^{-1})	A-Observed Peak-NC25 (cm^{-1})	Band position (cm^{-1})	Functional group
1	768.65	763.82	550-850	C-Cl alkyl halides stretch
2	1031.97	1031.93	990-1035	C-O valency vibration, C-O, C=C and C-C-O stretching
3	1507.4	1507.40	1442-1,516	Aliphatic C-H stretching, alkanes C-H scissoring and bending, Aromatic C-C ring stretching
4	2329.09	2324.26		
5	2883.63	2894.24	2860-2928	Aldehydes C-O stretches, esters, ketones, carboxylic acids
6	3328.23	3336.91	3200-3750	-OH stretching
7	3736.18	3743.90	3200-3750	-OH stretching

3.4. X-ray Diffraction (XRD) analysis

The XRD analysis is depicted in Figure 5. The diffractogram characteristics of the NC25 and SC25 showed cellulose identifier. This is strongly justified by the presence of peak at 2θ angles values around 16^0 and 22^0. These values are at proximity to the peak angle obtained by Poletto *et al.* [74] and Darmawan *et al.* [75], though at different intensities and curve widths. SC25 showed the highest intensity and the lower narrow curve width compared to NC25. This could be due to the more regular crystalline structure of cellulose in the corn cob obtained from South Africa. Along the 2θ angles values, there was a sudden spike (peak intensity) at 37.9 ^{0} and 44.1 ^{0} for NC25. This pattern seems to be most possibly due to the presence K_2CO_3 identifier based on the energy dispersive x-ray spectroscopy (EDX) which may have affected the variation of cellulose with 2θ angle values [76, 77]. The implication of this higher value of K_2CO_3 has been reported by Mueller-Hagedorn et al. [78] when they noted that the higher concentration of K_2CO_3 substantially reduced the peak decomposition while Klopper et al. [77] observed the promotion of cellulose pyrolysis effect and char formation due to the same compound. It is important to take cognizance of this effect in view of the need for bioresources integration.

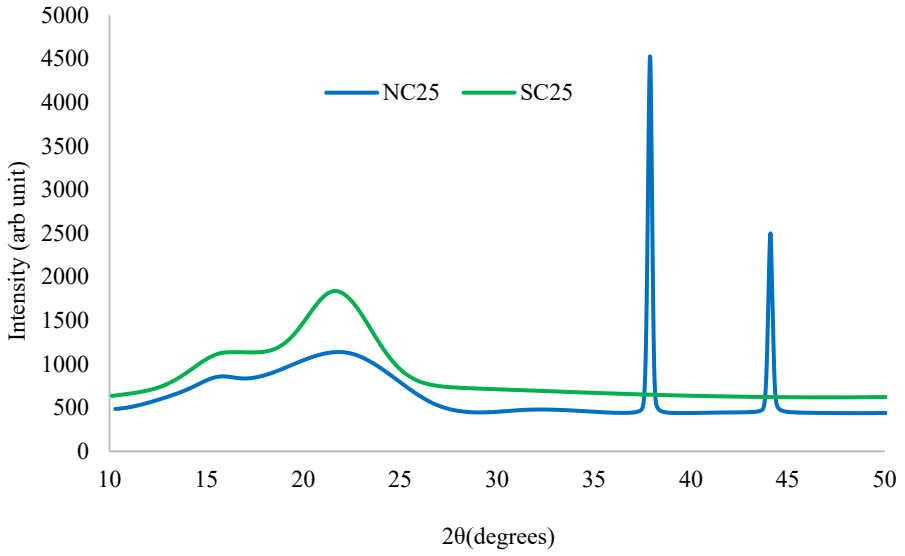

Figure 5: XRD analysis of corn cob.

3.5. Thermogravimetric analysis

Figure 6 shows the thermogravimetric (TG) and differential thermogravimetric (DTG) curves for pyrolysis of corn cob (NC25 and SC25) from different geospatial location at a heating rate of $10, 15, 30$ ℃ min^{-1} under inert (nitrogen) atmosphere. The heating rates was selected based on the optimal values which gave the high temperature resolution in the previous similar studies [79, 80]. The thermal characteristics of corn cob shows that the weight loss increases with temperature and the pyrolysis occur at three major stages (moisture drying, major degradation of less stable polymers and continuous devolatilization) which means that the process is a multistep reaction [35]. The first stage is clearly distinct from the other two stages of weight loss and it was noted at a

temperature range between 25 ℃ and 135 ℃ depending on the heating rate. The weight loss at this stage is also observed to be low (less than 10%) and it typifies the evaporation of absorbed cellular and surface moisture [32]. A separate peak was noted on DTG curve for this weigh loss zone, this may be as a result of loss of water and light volatiles in corn cob [79]. The second stage which is the active pyrolysis stage occurs between 250 ℃ and 450 ℃ where the weight loss of about 72% was noted, while the last stage occurs between 450 ℃ and progress to 750 ℃. At second stage, hemicellulose was the first to decompose due to its low degree of polymerization, and partial depolymerization reaction began for cellulose while the third stage which progress at less rapid rate typifies progressive decomposition of residual lignin and fixed carbon or degradation of complex high molecular weight component of corn cob [32].

The intersecting peaks for SC25 and NC25 at various heating rates is an indication of co-occurrence which means the two geospatial samples attain the same temperature and weight loss at a particular instance. This is significant for the co-pyrolysis of corn cob feedstock sourced from different locations as it determines the equilibrium weight loss at a particular temperature. It further indicates that the best performance maybe attained at this point of co-occurrence.

As the heating rate increases, the TG and DTG curves shift to higher temperature due to reducing thermal conductivity of the corn cob and consequential increase in time required for heat to be transferred within the corn cob matrix [81]. The reaction that should ordinarily occur at lower temperature takes place at higher temperature leading to heterogenous reaction distribution and different mass spectrum of the resultant product. However, an interesting situation occurred at the heating rate of 10 ℃ min^{-1} on the TG curve for SC25 toward the tail end of its thermal degradation. It was observed that 20% residue remained at around 800 ℃. This may be due to the complex thermal degradation behaviour of lignin and its associated linkage structure at low temperature. The phenomenon associated to this change in the residual mass can be interpreted by the fact that biomass has a heterogeneous structure, varying number of constituents and percentage composition [82]. These constituents display their characteristic individual degradation behaviour at a definite temperature range in the pyrolysis process. The lignin which is degraded at the last stage of the process has a complex thermal decomposition mechanism. The difference in the lignin composition of the corn cob sourced from different geospatial location may have resulted in different degradation rate which may have been amplified at low heating rate. Moreover, the cleavage of some linkages within the lignin matrix may have resulted in the formation of high reactive and unstable free radicals which may have further reacted through reorganisation and electron abstraction to form products with higher stability [83, 84] which can only be decomposed further at higher heating rate. The greater amount of this linkages may have been responsible for this interesting behaviour at low heating rate. On the other hand, the variation in the inorganic content affect the lignin decomposition leaving high amount of residue, whose condensed structures are not further degraded into low volatile compounds [85, 86] except at higher heating rate.

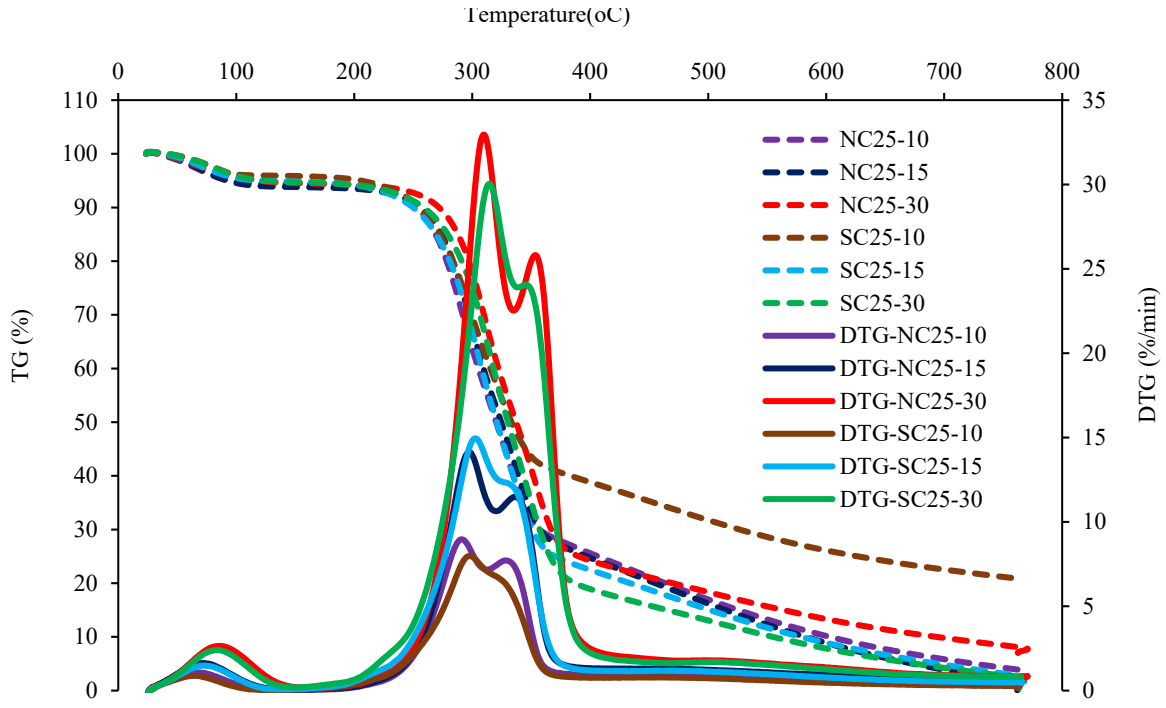

Figure 6: TG and DTG curve for NC25 and SC25 under nitrogen atmosphere

The average weight loss for SC25 is greater than NC25 at the heating rate of 30 ℃ min^{-1}. As previously stated, The stage two may be corresponding to the degradation of hemicellulose and cellulose [31, 34, 79] and the third stage is attributed to the decomposition of lignin. This observation is consistent with studies which have shown that the degradation of lignocellulosic biomass starts with hemicellulose, then cellulose and lignin in that order [80]. While there was only slight difference in DTG peaks for the two samples at the heating rate of 15 ℃ min^{-1}, notable difference in peak was observed at the heating rate of 30 ℃ min^{-1}. The maximum weight loss rate of SC25 was estimated 29.94%/min whereas NC25 has the highest maximum weight loss rate (32.94%/min) and lower peak temperature (310 ℃). This may be an indication of higher cellulose and hemicellulose composition in NC25 since the peak is higher in this sample.

3.6. Evaluation of kinetic parameters

Generally, TG kinetic data provides a mechanistic understanding of thermal cracking and can be upscaled to the high heating rate situation which is obtainable in the industry. The kinetic parameters which include activation energy and pre-exponential factor can be estimated from TG data. These parameters are important in the design of pyrolytic reactor because of the need to attain optimal conversion. As shown in Figure 7, temperature has positive effect on the conversion efficiency [87, 88] which determines the amount of product obtained at the end of the pyrolysis. The conversion efficiency increases with the temperature, although there is slight difference in temperature for each sample at a given conversions rate due to different heating rates.

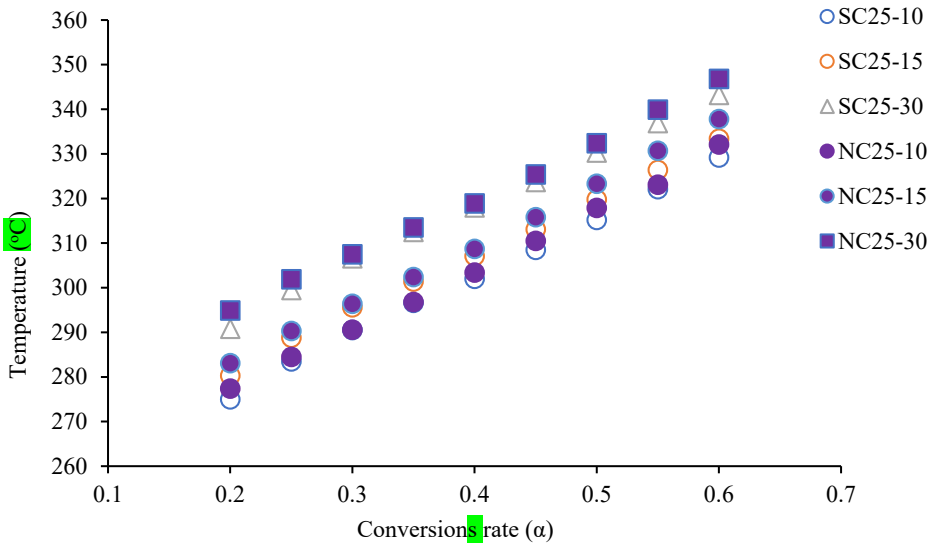

Figure 7: Temperature vs α curve at different heating rates.

Figure 8 shows the energy requirement for the conversion of corn cob to various pyrolysis products. Initially, low activation energy is required but it subsequently increases until it reaches conversions rate (α =0.5). Also, different inclination which was observed at the conversions rate (α =0.1) is an indication of different values of activation energy. This observation is similar to Alves et al. [34] which they reported for red microalgae. At α =0.5, the activation energy of NC25 begins to decrease while that of SC25 further increase for the two isothermal methods which were applied in this study. It is further noticed that the activation energy was the same for the NC25 and SC25 at an approximate conversions rate (α =0.375) and activation energy (E_a=175 kJmol^{-1}).

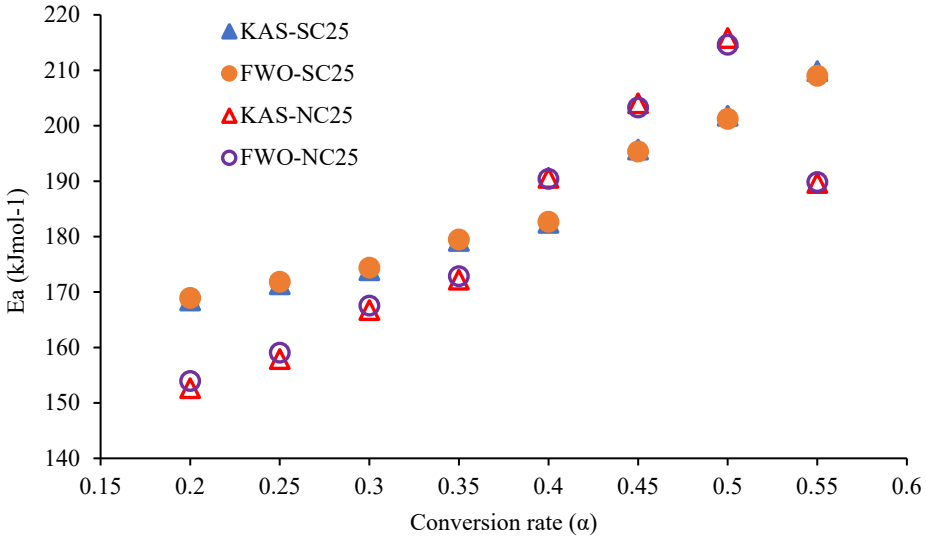

Figure 8: E_a vs α curve calculated based on FWO and KAS

The average E_a and k_0 for NC25 and SC25 based on FWO and KAS techniques are summarized in Table 8. ANOVA was carried out to show the effect of the geospatial location on the activation energy and pre-exponential factor of corn cob. At 95 % confidence level, the statistical difference between SC25 and NC25 was significant ($p = 7.61 \times 10^{-4}, F = 1312.2 > F_{crit} = 18.5$), but no significant difference was obtained for the pre-exponential factor ($p = 0.9222, F = 0.0122 < F_{crit} = 18.5128$). In order to establish the accuracy of the techniques, the correlation coefficient, R^2 was calculated, and it shows that the two methods are of high accuracy though FWO is slightly more accurate than KAS. There is a similarity in the average E_a obtained based on FWO and KAS for the same sample though these values are different for different samples (NC25 and SC25). Also, there is a notable difference between the pre-exponential factor, k_0. The highest value of E_a was estimated for SC25 (190.1 kJmol^{-1} and 189.9 kJmol^{-1}) for KAS and FWO methods respectively. k_0 is a constant characterized

by the nature of reaction and it is independent of temperature and the concentration of the substance. Based on FWO technique, NC25 has a narrow range of k_0 compared to SC25. Considering the suggestion by Maia and de Morais [89], k_0 above or below 10^9 s^{-1} is an indication of the end of complex reaction or a simple complex reaction respectively. Multistep decomposition process which was observed for the corn cob (NC25 and SC25) confirmed that there is complex chemical reaction which include the breaking of strong chemical bonds. k_0 values of NC25 and SC25 is higher than the those of wheat straw (2.59E+13 s^{-1}) ; Rice husk (1.57E+4 s^{-1}); and wheat straw pellets (6.25E+06 s^{-1}) determined using numerical solution [90] and it is lesser than, equal to or greater than the values for pea waste (3.34E+16-1.23E+28 s^{-1}) [91]. The effect of geospatial locations on pyrolysis was observed since the E_a and k_0 were different for the two samples. The implication of these values is that it will require more energy to decompose SC25 compared to NC25.

Table 8: Average E_a, k_0 and R^2 values of SC25 and NC25 based on FWO and Kissinger

Sample	**KAS**			**FWO**		
	E_a (kJmol^{-1})	k_0 (s^{-1})	R^2	E_a (kJmol^{-1})	k_0 (s^{-1})	R^2
NC25	185.9	4.65E+16	0.9980	186	3.77E+16	0.9982
SC25	190.1	9.46E+16	0.9768	189.9	7.26E+13	0.9773

3.7. Thermodynamic analysis

Thermodynamic parameters of the thermal degradation of corn cob (NC25 and SC25) in pyrolysis is presented in Table 9. The mean values of ΔG, ΔH, ΔS were 165.72 kJmol^{-1},185.28 kJmol^{-1}, and 33.88 Jmol^{-1}K^{-1} respectively for SC25 and 166.49 kJmol^{-1}, 190.40 kJmol^{-1}, and 34.02 Jmol^{-1}K^{-1} respectively for NC25. The value of the ΔS implies high reactivity and it further shows that less time is required for the formation of activation complex. The similar values of ΔG for SC25 and NC25 means that the pyrolysis process of the two samples require approximately the same amount of heat. This heat is lesser than what was obtained for some invasive aquatic microphytes (water hyacinth, ΔG~414.68 kJmol^{-1} and yellow velvetleaf, ΔG~359.43 kJmol^{-1}) [31] and pea waste (ΔG~ 143.20-147.80 kJmol^{-1}) [91] but greater than the values obtained for Lentinus edodes (pileus, ΔG~135.42 kJmol^{-1} and stipes, ΔG~ 129.04 kJmol^{-1}) [32] and spend mushroom substrate (ΔG~ 146.18-147.80 kJmol^{-1}) [33]. The lower ΔG shows that the pyrolytic reaction occurs with less energy requirement.

Table 9: Thermodynamic parameters of SC and NC based on FWO at 15K/min

Sample	SC25			NC25		
α	ΔH (kJmol^{-1})	ΔG (kJmol^{-1})	ΔS(Jmol^{-1}K^{-1})	ΔH (kJmol^{-1})	ΔG (kJmol^{-1})	ΔS(Jmol^{-1}K^{-1})
0.20	163.85	157.08	11.73	153.94	158.70	-8.32
0.25	166.70	159.74	12.07	159.06	160.61	-2.71
0.30	169.20	161.90	12.65	167.54	162.15	9.40
0.35	174.41	163.66	18.63	172.86	163.93	15.60
0.40	177.63	165.39	21.20	190.40	165.70	43.13
0.45	190.83	167.27	40.80	203.28	168.04	61.51
0.50	196.85	169.57	47.26	214.61	170.74	76.58
0.55	204.84	171.99	56.90	189.83	172.48	30.28
0.60	223.18	174.89	83.65	222.37	176.10	80.75
Average	**185.28**	**165.72**	**33.88**	**185.99**	**166.49**	**34.02**

4. Conclusion

This study presents an important contribution to further the discuss on the regional integration of bioresources. The state of affair regarding the regional integration of bioresources were first discussed. Since the integration of biomass from different regional locations depend on detailed understanding of the physico-chemical properties and other parameters that are crucial to its utilization. The physico-chemical properties and thermodynamic parameters of corn cob sourced from two different geospatial locations in Africa were analysed under identical conditions. The thermal decomposition of both corn cob sourced from Nigeria (NC25) and South Africa (SC25)

exhibited an identical characteristics except at 30 ℃ min^{-1} where some disparities in the thermodynamic behaviour and energy parameters were observed. The thermodynamic and kinetic parameters are sources of useful information which could be deployed in the simulation, optimization and scaling-up of the bio-reactors for pyrolysis process. There were statistically significant differences in elemental composition, surface properties and activation energy. This further suggests that the geospatial location from where the biomass is sourced may have an impact on the properties. The results obtained further confirmed the feasibility of corn cob as a feedstock toward renewable energy generation while also reinforcing the possibility of co-combustion of similar feedstock from different geospatial locations. The investigation of different atmosphere for TGA analysis and different probe gases for surface properties characterisation is suggested for further research. Also, similar studies like this but including other neighbouring countries with potential bioresources could be considered for regional integration. Utmostly, a model which predicts the optimal co-pyrolytic performance of corn cob and other bioresources toward energy sustainability can be developed.

References

[1] Worldometers, "Population of Africa," *http://www.worldometers.info/world-population/africa-population/ accessed on 13/03/2019,* 2019.

[2] K. Hashimoto, "Current Situation of Energy Consumption and Carbon Dioxide Emissions of Our World," in *Global Carbon Dioxide Recycling*: Springer, 2019, pp. 25-31.

[3] V. Lizunkov, E. Politsinskaya, E. Malushko, A. Kindaev, and M. Minin, "Population of the world and regions as the principal energy consumer," *International journal of energy economics and policy,* vol. 8, no. 3, pp. 250-257, 2018.

[4] V. Smil, *Energy in world history*. Routledge, 2019.

[5] J. Rockström, O. Gaffney, J. Rogelj, M. Meinshausen, N. Nakicenovic, and H. J. Schellnhuber, "A roadmap for rapid decarbonization," *Science,* vol. 355, no. 6331, pp. 1269-1271, 2017.

[6] G. Perin and T. Morosinotto, "Potential of Microalgae Biomass for the Sustainable Production of Bio-commodities," 2019.

[7] P. A. Adedeji, S. Akinlabi, N. Madushele, and O. O. Olatunji, "Towards low-carbon energy state in South Africa: a survey of energy availability and sustainability," 2019.

[8] P. McKendry, "Energy production from biomass (part 1): overview of biomass," *Bioresource technology,* vol. 83, no. 1, pp. 37-46, 2002.

[9] P. Bajpai, "Fuel Potential of Third Generation Biofuels," in *Third Generation Biofuels*: Springer, 2019, pp. 7-10.

[10] Y. D. Singh, P. Mahanta, and U. Bora, "Comprehensive characterization of lignocellulosic biomass through proximate, ultimate and compositional analysis for bioenergy production," *Renewable Energy,* vol. 103, pp. 490-500, 2017.

[11] O. Olatunji *et al.*, "Electric Power Crisis in Nigeria: A Strategic Call for Change of Focus to Renewable Sources," *IOP Conference Series: Materials Science and Engineering,* vol. 413, no. 1, p. 012053, 2018.

[12] I. m. fund(IMF), "World economy outlook database, April 2018," *https://www.imf.org/en/publications/weo accessed on 15th January 2019,* 2018.

[13] A. A. Awoyale and D. Lokhat, "Harnessing the potential of bio-ethanol production from lignocellulosic biomass in Nigeria–a review," *Biofuels, Bioproducts and Biorefining,* vol. 13, no. 1, pp. 192-207, 2019.

[14] U. Nzotcha and J. Kenfack, "Contribution of the wood-processing industry for sustainable power generation: Viability of biomass-fuelled cogeneration in Sub-Saharan Africa," *Biomass and bioenergy,* vol. 120, pp. 324-331, 2019.

[15] Worldbank, "GDP for South Africa and Nigeria," *https://data.worldbank.org/?locations=ZA-N acessed on 28/08/2019,* 2018.

[16] J. Ben-Iwo, V. Manovic, and P. Longhurst, "Biomass resources and biofuels potential for the production of transportation fuels in Nigeria," *Renewable and Sustainable Energy Reviews,* vol. 63, pp. 172-192, 2016.

[17] S. Paul, A. Dutta, M. Thimmanagari, and F. Defersha, "Techno-economic assessment of corn stover for hybrid bioenergy production: A sustainable approach," *Case Studies in Thermal Engineering,* vol. 13, p. 100408, 2019.

[18] L. M. Mohlala, M. O. Bodunrin, A. A. Awosusi, M. O. Daramola, N. P. Cele, and P. A. Olubambi, "Beneficiation of corncob and sugarcane bagasse for energy generation and materials development in Nigeria and South Africa: A short overview," *Alexandria Engineering Journal,* vol. 55, no. 3, pp. 3025-3036, 2016.

[19] F. a. A. O. o. t. U. N. FAO, "FAOSTAT-CROPS," *http://www.fao.org/faostat/en/#data/QC accessed on 09/04/2019,* 2019.

[20] J. H. Leal, C. M. Moore, A. D. Sutton, and T. A. Semelsberger, "Surface energy of air fractionated corn stover," *Industrial Crops and Products,* vol. 137, pp. 628-635, 2019.

[21] O. O. Olatunji, O. Ajayi, P. Mashinini, and M. Nkosinathi, "Experimental investigation of thermal properties of Lignocellulosic biomass: A review," *IOP Conference Series: Materials Science and Engineering,* vol. 413, no. 1, p. 012054, 2018.

[22] S. V. Vassilev, D. Baxter, L. K. Andersen, and C. G. Vassileva, "An overview of the chemical composition of biomass," *Fuel,* vol. 89, no. 5, pp. 913-933, 2010.

[23] O. O. Olatunji, S. A. Akinlabi, M. P. Mashinini, S. O. Fatoba, and O. O. Ajayi, "Thermo-gravimetric characterization of biomass properties: A review," *IOP Conference Series: Materials Science and Engineering,* vol. 423, no. 1, p. 012175, 2018.
[24] C. L. Williams, T. L. Westover, R. M. Emerson, J. S. Tumuluru, and C. Li, "Sources of biomass feedstock variability and the potential impact on biofuels production," *BioEnergy Research,* vol. 9, no. 1, pp. 1-14, 2016.
[25] H. T. Huynh, J. Hufnagel, A. Wurbs, and S. D. Bellingrath-Kimura, "Influences of soil tillage, irrigation and crop rotation on maize biomass yield in a 9-year field study in Müncheberg, Germany," *Field Crops Research,* vol. 241, p. 107565, 2019.
[26] X. Yao, K. Xu, and Y. Liang, "Assessing the Effects of Different Process Parameters on the Pyrolysis Behaviors and Thermal Dynamics of Corncob Fractions," *BioResources,* vol. 12, no. 2, pp. 2748-2767, 2017.
[27] M. E. Mostafa *et al.*, "The significance of pelletization operating conditions: An analysis of physical and mechanical characteristics as well as energy consumption of biomass pellets," *Renewable and Sustainable Energy Reviews,* vol. 105, pp. 332-348, 2019.
[28] D. Djatkov, M. Martinov, and M. Kaltschmitt, "Influencing parameters on mechanical–physical properties of pellet fuel made from corn harvest residues," *Biomass and bioenergy,* vol. 119, pp. 418-428, 2018.
[29] Y. Xu and B. Chen, "Investigation of thermodynamic parameters in the pyrolysis conversion of biomass and manure to biochars using thermogravimetric analysis," *Bioresource technology,* vol. 146, pp. 485-493, 2013.
[30] V. Dhyani and T. Bhaskar, "A comprehensive review on the pyrolysis of lignocellulosic biomass," *Renewable Energy,* vol. 129, pp. 695-716, 2018.
[31] J. L. F. Alves, J. C. G. da Silva, V. F. da Silva Filho, R. F. Alves, W. V. de Araujo Galdino, and R. F. De Sena, "Kinetics and thermodynamics parameters evaluation of pyrolysis of invasive aquatic macrophytes to determine their bioenergy potentials," *Biomass and bioenergy,* vol. 121, pp. 28-40, 2019.
[32] H. Zou, F. Evrendilek, J. Liu, and M. Buyukada, "Combustion behaviors of pileus and stipe parts of Lentinus edodes using thermogravimetric-mass spectrometry and Fourier transform infrared spectroscopy analyses: Thermal conversion, kinetic, thermodynamic, gas emission and optimization analyses," *Bioresource technology,* vol. 288, p. 121481, 2019.
[33] J. Huang *et al.*, "Combustion behaviors of spent mushroom substrate using TG-MS and TG-FTIR: Thermal conversion, kinetic, thermodynamic and emission analyses," *Bioresource technology,* vol. 266, pp. 389-397, 2018.
[34] J. L. F. Alves *et al.*, "Bioenergy potential of red macroalgae Gelidium floridanum by pyrolysis: Evaluation of kinetic triplet and thermodynamics parameters," *Bioresource technology,* vol. 291, p. 121892, 2019.
[35] A. Mlonka-Mędrala, A. Magdziarz, T. Dziok, M. Sieradzka, and W. Nowak, "Laboratory studies on the influence of biomass particle size on pyrolysis and combustion using TG GC/MS," *Fuel,* vol. 252, pp. 635-645, 2019.
[36] H. L. Lam, P. Varbanov, and J. Klemeš, "Minimising carbon footprint of regional biomass supply chains," *Resources, Conservation and Recycling,* vol. 54, no. 5, pp. 303-309, 2010.
[37] J.-M. Li, A.-H. Li, P. S. Varbanov, and Z.-Y. Liu, "Distance potential concept and its applications to the design of regional biomass supply chains and solving vehicle routing problems," *Journal of cleaner production,* vol. 144, pp. 426-436, 2017.
[38] L. Nunes, T. Causer, and D. Ciolkosz, "Biomass for energy: A review on supply chain management models," *Renewable and Sustainable Energy Reviews,* vol. 120, p. 109658, 2020.
[39] M. A. Sharara *et al.*, "Sustainable feedstock for bioethanol production: impact of spatial resolution on the design of a sustainable biomass supply-chain," *Bioresource Technology,* p. 122896, 2020.
[40] E. Commission, "A sustainable bioeconomy for Europe: Strengthening the connection between economy, society and the environment," 2018.
[41] M. Rodríguez and J. A. Camacho, "The development of trade of biomass in Spain: A raw material equivalent approach," *Biomass and Bioenergy,* vol. 133, p. 105450, 2020.
[42] D. Hadebe, A. Hansa, C. Ndlhovu, and M. Kibido, "Scaling Up Renewables Through Regional Planning and Coordination of Power Systems in Africa—Regional Power System Planning to Harness Renewable Resources and Diversify Generation Portfolios in Southern Africa," *Current Sustainable/Renewable Energy Reports,* vol. 5, no. 4, pp. 224-229, 2018.
[43] ASTM, "Standard test methods," *https://www.astm.org accessed on 30th April, 2018,* 2017.
[44] A. E872-82, "Standard test method for volatile matter in the analysis of particulate wood fuels. West Conshohocken, PA: ASTM International," 2013.
[45] A. E1756-08, "Standard test method for determination of total solids in biomass. West Conshohocken, PA: ASTM International; ," 2015.
[46] A. E1755-01, "Standard test method for ash in biomass. West Conshohocken, PA: ASTM International," 2015.
[47] A. E1757-01, "Standard Practice for Preparation of Biomass for Compositional Analysis," *PA: America society for Testing materilas, International,* 2015.
[48] ASTM, "E1755 Standard Test Method for Ash in Biomass," *America Society of Testing Materials, International,* 2015.
[49] R. García, C. Pizarro, A. G. Lavín, and J. L. Bueno, "Spanish biofuels heating value estimation. Part II: Proximate analysis data," *Fuel,* vol. 117, pp. 1139-1147, 2014.
[50] J. B. Sluiter, R. O. Ruiz, C. J. Scarlata, A. D. Sluiter, and D. W. Templeton, "Compositional analysis of lignocellulosic feedstocks. 1. Review and description of methods," *J Agric Food Chem,* vol. 58, no. 16, pp. 9043-53, Aug 25 2010.
[51] D. D. S. P. L. DDS, "Eco Operating Manual," *http://www.ddscalorimeters.com/ accessed on 28/11/2018,* 2018.
[52] S. Brunauer, P. H. Emmett, and E. Teller, "Adsorption of gases in multimolecular layers," *Journal of the American chemical society,* vol. 60, no. 2, pp. 309-319, 1938.

[53] D. Zhang and R. Luo, "Modifying the BET model for accurately determining specific surface area and surface energy components of aggregates," *Construction and Building Materials,* vol. 175, pp. 653-663, 2018.
[54] Q. Che *et al.*, "Influence of physicochemical properties of metal modified ZSM-5 catalyst on benzene, toluene and xylene production from biomass catalytic pyrolysis," *Bioresource Technology,* 2019.
[55] Y. C. Feng, Y. Meng, F. X. Li, Z. P. Lv, and J. W. Xue, "Synthesis of mesoporous LTA zeolites with large BET areas," *Journal of Porous Materials,* vol. 20, no. 3, pp. 465-471, 2013.
[56] M. v. Crystal-Impact, *http://www.crystalimpact.com/match/,* 2013.
[57] T. Akahira, "Trans. Joint convention of four electrical institutes," *Res. Rep. Chiba Inst. Technol.,* vol. 16, pp. 22-31, 1971.
[58] H. E. Kissinger, "Reaction kinetics in differential thermal analysis," *Analytical chemistry,* vol. 29, no. 11, pp. 1702-1706, 1957.
[59] C. D. Doyle, "Kinetic analysis of thermogravimetric data," *Journal of applied polymer science,* vol. 5, no. 15, pp. 285-292, 1961.
[60] B. Biswas, N. Pandey, Y. Bisht, R. Singh, J. Kumar, and T. Bhaskar, "Pyrolysis of agricultural biomass residues: Comparative study of corn cob, wheat straw, rice straw and rice husk," *Bioresource technology,* vol. 237, pp. 57-63, 2017.
[61] A. Demirbaş, "Calculation of higher heating values of biomass fuels," *Fuel,* vol. 76, no. 5, pp. 431-434, 1997.
[62] N. Gómez, J. G. Rosas, J. Cara, O. Martínez, J. A. Alburquerque, and M. E. Sánchez, "Slow pyrolysis of relevant biomasses in the Mediterranean basin. Part 1. Effect of temperature on process performance on a pilot scale," *Journal of cleaner production,* vol. 120, pp. 181-190, 2016.
[63] L. Brinchi, F. Cotana, E. Fortunati, and J. Kenny, "Production of nanocrystalline cellulose from lignocellulosic biomass: technology and applications," *Carbohydrate Polymers,* vol. 94, no. 1, pp. 154-169, 2013.
[64] S. Channiwala and P. Parikh, "A unified correlation for estimating HHV of solid, liquid and gaseous fuels," *Fuel,* vol. 81, no. 8, pp. 1051-1063, 2002.
[65] A. Demirbas, D. Gullu, A. Caglar, and F. Akdeniz, "Estimation of calorific values of fuels from lignocellulosics," *Energy Sources,* vol. 19, no. 8, pp. 765-770, 1997.
[66] J. Parikh, S. Channiwala, and G. Ghosal, "A correlation for calculating HHV from proximate analysis of solid fuels," *Fuel,* vol. 84, no. 5, pp. 487-494, 2005.
[67] A. Barakat, C. Mayer-Laigle, A. Solhy, R. A. Arancon, H. De Vries, and R. Luque, "Mechanical pretreatments of lignocellulosic biomass: towards facile and environmentally sound technologies for biofuels production," *Rsc Advances,* vol. 4, no. 89, pp. 48109-48127, 2014.
[68] S. Zu *et al.*, "Pretreatment of corn stover for sugar production using dilute hydrochloric acid followed by lime," *Bioresource technology,* vol. 152, pp. 364-370, 2014.
[69] W. de Jong, "Biomass Composition, Properties, and Characterization," *Biomass as a Sustainable Energy Source for the Future: Fundamentals of Conversion Processes,* pp. 36-68, 2014.
[70] T. Ji *et al.*, "Green processing of plant biomass into mesoporous carbon as catalyst support," *Chemical Engineering Journal,* vol. 295, pp. 301-308, 2016.
[71] C. J. Mena-Durán, P. Quintana, R. Barbosa, J. Baas, and B. Escobar, "Characteristics of Hydrochars Prepared from Cassava Residues Using Different Aqueous Media," *Waste and Biomass Valorization,* pp. 1-6, 2019.
[72] Merck, "IR Spectrum Table & Chart," *https://www.sigmaaldrich.com/technical-documents/articles/biology/ir-spectrum-table.html accessed 8th March 2019.,* 2019.
[73] S. Kubo and J. F. Kadla, "Hydrogen bonding in lignin: a Fourier transform infrared model compound study," *Biomacromolecules,* vol. 6, no. 5, pp. 2815-2821, 2005.
[74] M. Poletto, A. J. Zattera, M. M. Forte, and R. M. Santana, "Thermal decomposition of wood: Influence of wood components and cellulose crystallite size," *Bioresource Technology,* vol. 109, pp. 148-153, 2012.
[75] S. Darmawan, N. J. Wistara, G. Pari, A. Maddu, and W. Syafii, "Characterization of lignocellulosic biomass as raw material for the production of porous carbon-based materials," *BioResources,* vol. 11, no. 2, pp. 3561-3574, 2016.
[76] L. A. De Macedo, J.-M. Commandré, P. Rousset, J. Valette, and M. Pétrissans, "Influence of potassium carbonate addition on the condensable species released during wood torrefaction," *Fuel Processing Technology,* vol. 169, pp. 248-257, 2018.
[77] L. Klopper, C. Strydom, and J. Bunt, "Influence of added potassium and sodium carbonates on CO2 reactivity of the char from a demineralized inertinite rich bituminous coal," *Journal of analytical and applied pyrolysis,* vol. 96, pp. 188-195, 2012.
[78] M. Müller-Hagedorn, H. Bockhorn, L. Krebs, and U. Müller, "A comparative kinetic study on the pyrolysis of three different wood species," *Journal of analytical and Applied Pyrolysis,* vol. 68, pp. 231-249, 2003.
[79] A. Kumar, L. Wang, Y. A. Dzenis, D. D. Jones, and M. A. Hanna, "Thermogravimetric characterization of corn stover as gasification and pyrolysis feedstock," *Biomass and Bioenergy,* vol. 32, no. 5, pp. 460-467, 2008.
[80] S. A. El-Sayed and M. Khairy, "Effect of heating rate on the chemical kinetics of different biomass pyrolysis materials," *Biofuels,* vol. 6, no. 3-4, pp. 157-170, 2015/07/04 2015.
[81] T. Kan, V. Strezov, and T. Evans, "Effect of the heating rate on the thermochemical behavior and biofuel properties of sewage sludge pyrolysis," *Energy & Fuels,* vol. 30, no. 3, pp. 1564-1570, 2016.
[82] H. Haykiri-Acma, S. Yaman, and S. Kucukbayrak, "Effect of heating rate on the pyrolysis yields of rapeseed," *Renewable Energy,* vol. 31, no. 6, pp. 803-810, 2006/05/01/ 2006.
[83] A. Afifi, J. Hindermann, E. Chornet, and R. Overend, "The cleavage of the aryl□ O□ CH3 bond using anisole as a model compound," *Fuel,* vol. 68, no. 4, pp. 498-504, 1989.
[84] M. Brebu and C. Vasile, "Thermal degradation of lignin—a review," *Cellulose Chemistry & Technology,* vol. 44, no. 9, p. 353, 2010.

[85] G. Dobele, G. Rossinskaja, T. Dizhbite, G. Telysheva, D. Meier, and O. Faix, "Application of catalysts for obtaining 1, 6-anhydrosaccharides from cellulose and wood by fast pyrolysis," *Journal of Analytical and Applied Pyrolysis,* vol. 74, no. 1-2, pp. 401-405, 2005.
[86] C. Di Blasi, C. Branca, and A. Galgano, "Effects of diammonium phosphate on the yields and composition of products from wood pyrolysis," *Industrial & engineering chemistry research,* vol. 46, no. 2, pp. 430-438, 2007.
[87] K. P. Shadangi and K. Mohanty, "Comparison of yield and fuel properties of thermal and catalytic Mahua seed pyrolytic oil," *Fuel,* vol. 117, pp. 372-380, 2014.
[88] D. Pradhan, R. Singh, H. Bendu, and R. Mund, "Pyrolysis of Mahua seed (Madhuca indica)–Production of biofuel and its characterization," *Energy conversion and management,* vol. 108, pp. 529-538, 2016.
[89] A. A. D. Maia and L. C. de Morais, "Kinetic parameters of red pepper waste as biomass to solid biofuel," *Bioresource Technology,* vol. 204, pp. 157-163, 2016.
[90] A. Álvarez, C. Pizarro, R. García, J. Bueno, and A. Lavín, "Determination of kinetic parameters for biomass combustion," *Bioresource technology,* vol. 216, pp. 36-43, 2016.
[91] E. Müsellim, M. H. Tahir, M. S. Ahmad, and S. Ceylan, "Thermokinetic and TG/DSC-FTIR study of pea waste biomass pyrolysis," *Applied Thermal Engineering,* vol. 137, pp. 54-61, 2018.